HHS Public Access

Author manuscript

Acta Otolaryngol. Author manuscript; available in PMC 2019 April 01.

Published in final edited form as:

Acta Otolaryngol. 2018 April ; 138(4): 367–374. doi:10.1080/00016489.2017.1395515.

Optical assessment of the *in vivo* tympanic membrane status using a handheld optical coherence tomography-based otoscope

Kibeom Park[a], **Nam Hyun Cho**[b,c,iD], **Mansik Jeon**[a], **Sang Heun Lee**[d,iD], **Jeong Hun Jang**[e,iD], **Stephen A. Boppart**[f,g], **Woonggyu Jung**[h,iD], and **Jeehyun Kim**[a,iD]

[a]School of Electronics Engineering, College of IT Engineering, Kyungpook National University, Daegu, Korea

[b]Eaton-Peabody Laboratories, Massachusetts Eye and Ear Infirmary (MEEI), Boston, MA, USA

[c]Department of Otology and Laryngology, Harvard Medical School, Boston, MA, USA

[d]Department of Otorhinolaryngology, Daegu Veterans Hospital, Daegu, Korea

[e]Department of Otorhinolaryngology, College of Medicine, Ajou University, Suwon, Korea

[f]Department of Electrical and Computer Engineering, University of Illinois at Urbana-Champaign, Urbana, IL, USA

[g]Beckman Institute for Advanced Science, Urbana, IL, USA

[h]School of Nano-Bioscience and Chemical Engineering, School of Electrical and Computer Engineering, Ulsan National Institute of Science and Technology, Ulsan, Korea

Abstract

Objective—Conventional otoscopes and oto-endoscopes, which are used to examine the tympanic membrane (TM), do not provide tomographic information. Optical coherence tomography (OCT) non-invasively reveals the depth-resolved internal microstructure of the TM with very high spatial resolution. We designed this study to examine the TMs with middle ear diseases using a handheld otoscope employing 860 nm spectral domain (SD)-OCT, combined with video camera and to demonstrate the clinical applicability of this system.

Design—A total of 120 patients with otologic symptoms were enrolled. TM images were obtained using the handheld OCT-based otoscope (860 nm central wave length, 15 μm axial resolution, 15 μm lateral resolution, and 7 mm scanning range using relay lens). Both OCT and

CONTACT Jeong Hun Jang, jhj@ajou.ac.kr, Department of Otorhinolaryngology-Head and Neck Surgery, Ajou University, College of Medicine, 164 World Cup-ro, Yeongtong-gu, Suwon 443-380, Korea.

ORCID

Nam Hyun Cho http://orcid.org/0000-0003-2653-779X
Sang Heun Lee http://orcid.org/0000-0002-4860-4386
Jeong Hun Jang http://orcid.org/0000-0003-1707-5714
Woonggyu Jung http://orcid.org/0000-0001-7424-3679
Jeehyun Kim http://orcid.org/0000-0003-1217-9338

Disclosure statement

No potential conflict of interest was reported by the authors.

oto-endoscope images were compared according to the clinical characteristics such as perforation, retraction, and postoperative healing process.

Results—The objective grade about the thickness of perforation margins and the accurate information about the extent of TM retraction that was not distinguishable by oto-endoscopic exam could be identified using this system. The postoperative healing process of TMs could be also followed using the OCT device.

Conclusion—These analyses from the surgeon-oriented perspective suggest another useful application of the handheld OCT device.

Keywords

Optical coherence tomography; tympanic membrane; otitis media; otoscope

Introduction

Otitis media (OM), defined as inflammation of the middle ear, is one of the most common diseases managed in otorhinolaryngology. OM is further classified as acute OM (AOM), OM with effusion (OME), and chronic OM (COM). AOM is an acute infection/inflammation of the middle ear mucosa which also involves the mastoid air cells. The cumulative incidence of the first episode of AOM is 80% by 3 years of age [1]. OM with effusion (OME) occurs when fluid collects within the middle ear space as a result of the negative pressure produced by altered Eustachian tube function. The prevalence of OME is 6.8% for all children, decreasing with age from 12.9% in children 5–6 years old to 3% among those 13–14 years old [2]. AOM and OME are treated medically (antibiotics) and surgically (myringotomy and tympanostomy tube insertion) according to the clinical practice guideline such as American academy of pediatrics and American academy of family physicians guideline [3,4]. COM is a permanent abnormality on the tympanic membrane following a long-standing middle ear infection emanating from previous AOM, OME, or negative pressure to the middle ear. Pathologically, COM is subdivided into mucosal COM and squamous COM. Mucosal COM results from a perforation in the tympanic membrane (TM), which allows the middle ear to become chronically infected, leading to mucosal hypertrophy and discharge. Squamous COM encompasses retraction pocket of TM and cholesteatoma which is a cystic, inflammatory mass keratinizing stratified squamous epithelium. The prevalence of COM is less than 4% in the mucosal type [5] and various according to race in the squamous type. The principles of COM management entail eradication of disease and restoration of function. Aural toileting and appropriate antibiotics (topical and systemic) are prerequisite to active inflammation control and surgical procedures such as tympanomastoidectomy could be performed.

The otoscope is a standard and reliable diagnostic tool for OM as it can be utilized easily in the initial evaluation of OM. However, the sensitivity and the specificity of otoscopic TM examinations are limited by factors such as improper speculum size, physician skills, and patient cooperation. Furthermore, structures within the middle ear cannot be visualized using a conventional otoscope, even in cases of TM with inflammatory change. Recently, oto-endoscopes have become popular for a thorough evaluation of the TM, but the information

that they provide about the middle ear cavity inside the TM remains limited, which is the main drawback of such devices.

Optical coherence tomography (OCT) is a real-time optical imaging method that non-invasively acquires detailed images of *in vivo* tissues based on optical interference. It is non-destructive and harmless because it uses low-power and a broadband near-infrared light source. The high-resolution tomographic images acquired with OCT cannot be obtained with traditional tomography equipment. The technique has been used mainly in ophthalmology and dermatology because of the easy application of OCT systems without additional devices such as scanners and endoscopes. Recently, the applicability of OCT systems in otology has also been reported. Through studies demonstrating OCT as a diagnostic tool for middle ear diseases in clinical and animal studies, the scanning depth became much longer, the scanning range wider, and the images were acquired in nearly real time [6,7]. With the addition of vibrometry mode, the vibration of middle ear structures in response to sound could be measured as well [8].

Compared with otoscopic and oto-endoscopic examinations, OCT imaging provides the clinician with real-time cross-sectional information about the TM and thus is a powerful diagnostic tool to delineate tissue pathology at micro-scale resolution. The image resolution (10 μm) is sufficient to generate detailed images of a quality that allows screening of the TM. Moreover, the resolution significantly exceeds that of traditional CT (300 μm) and 3T-magnetic resonance imaging ($1 \times 1 \times 1$ mm^3) [9,10]. Unlike high-frequency ultrasound (150 μm), OCT imaging can be performed in either direct or near contact, without the use of an impedance or refractive index matching gel, yielding higher-resolution images, albeit with a moderate sacrifice of imaging depth [10].

A handheld OCT device with a design similar to that of a traditional otoscope is now available [11]. Recently, we updated this system by adding a relay lens, which improved the device as a next-generation middle ear diagnostic tool. In this system, a video camera is integrated into the OCT to guide the device towards the TM through the external auditory canal (EAC) and localize the region of interest. Both the video camera image and the real-time OCT image of TM can be projected simultaneously on a computer monitor. This study was designed to image the TMs of patients with OM using OCT and thereby demonstrate the utility of this system as a diagnostic tool in otorhinolaryngology clinics.

Materials and methods

Patients

This study was approved by the institutional review board of the Clinical Research Institute in Kyungpook National University Hospital (IRB no. 2012-12-006). The 120 enrolled patients with otologic symptoms, including otorrhea and hearing impairment, were assessed at the Department of Otorhinolaryngology at Kyungpook National University Hospital. Medical records, oto-endoscopic findings, and temporal bone CT findings were reviewed. The characteristics of the patients are shown in Table 1.

OCT system

Figure 1 presents a schematic of the system. The broadband light source is a super-luminescent diode (SLED) operating in high-power mode (SLD-35-HP, Superlum Ltd., Pasadena, CA). The SLED has a center wavelength of 860 nm and a spectrum with a full width at half-maximum of 65 nm. The beam from the SLED is coupled to two fiber-based Michelson interferometers via a 50:50 fiber-fused coupler (FC850-40-50-APC, Thorlabs, Pasadena, CA). The light in each interferometer is split between the sample and the reference arms. The reference path of the system contains a dispersion compensation unit (prism pair) to account for the dispersion within the optics of the sample path. For the sample arm, the handheld probe is implemented with all optics, including a collimator, galvanometer scanner, magnifier lens, relay lens, and miniaturized charge-coupled device camera-based color video with 1.3 megapixels. The handheld probe has a 2-m-long optical fiber and electrical wires, allowing the clinician to diagnose patients while keeping them comfortable. The minimized handheld OCT probe is similar in size to a conventional otoscope and can be readily used as a diagnostic tool. For the detection arm of the spectral domain (SD) OCT system, the reflected light from the sample and reference arms was collimated and detected by a spectrometer, which consisted of a transmission-type diffraction grating (spatial frequency: 1800 lpmm, nominal AOI/AOD: 46.05°, Wasatch Photonics, West Logan, UT), an objective lens (f = 100 mm) and a 12-bit complementary metal-oxide-semiconductor line-scanning camera (spL4096-140k; Basler AG, Ahrensburg, Germany) with an effective line rate of 70,000 lines/s. The point spread function was inspected and its distortion compensated. The resolution and the signal-to-noise ratio were improved by implementing an accurate spectral calibration method. The measured axial resolution of the system was 6 μm in air at an imaging depth of 50 μm; the measured lateral resolution at zero depth was 15 μm.

The system's processing method was detailed in the study by Cho et al. [12]. In brief, all processing was performed using LabVIEW (Aachen, Germany). After its detection by the camera, the interfered signal is transferred towards the Central Processing Unit (CPU) through the frame grabber (PCIe-1433). We adopted the Graphics Processing Unit (GPU) to provide fast image processing and display. This allowed us to implement the real-time display feature after massive data processing, including interpolation to ensure full-range k-domain linearization as well as fast Fourier transform and log-scaling processes. Background noise removal to minimize any speckle in the source is performed by determining the difference between the B-scan data acquired by the existing OCT and new OCT system signals. The reconstructed OCT images are transferred back to the host memory to be displayed in real time. The speed of the system is 100 frames/s in the SD-OCT system with an image size of 2048 × 512 pixels.

In the conventional system, the scanning range is strictly limited to the specula tip. To extend the scanning range to a larger field, we inserted a relay lens between the galvanometer and the focusing lens. The probe was designed by considering the ear-specula tip diameter and the distance of the TM from the system. The focal lengths of the relay lens are 19 and 35 mm, and the focusing distance of the corresponding focal lens 50 mm. Thus, as shown in Figure 1(B), after the beam is propagated from the galvanometer, relay lens,

focusing lens, and specula, it focuses on and then scans the sample, thus overcoming the limits of the scanning range. Our handheld OCT probe has the ability to image a wide field of view on the TM. The scanning range of 7 mm is greater than that of the conventional method, which is 2–3 mm. Figure 1(C) shows the OCT image of the TM, which was scanned over a scanning range of ~2 mm using the conventional OCT system. Figure 1(D) shows the OCT images of a widely scanned area also acquired using the newly developed system. The relay lens of the handheld probe enhances the lateral scanning range up to 7 mm, which is ~3.5 larger than that of a system without a relay lens.

Imaging

Imaging was carried out by inserting the handheld probe into the EAC under video camera guidance and placing it directly in front of the TM. With the aid of an indicator in the video camera, two-dimensional (2D) images of the whole TM were acquired to identify regions of interest. Repeated images of abnormal regions were then taken. The imaging time was <5 min per patient. A low-coherence interferometry (LCI) scan, which is an optical imaging technique capable of measuring one-dimensional depth-resolved tissue structure, was acquired for specified regions after image processing. Using LCI, TM thickness can be estimated and structural information obtained. Prior to the acquisition of OCT image, the status of TM was evaluated and diagnosed using the oto-endoscope.

Data analysis

The reliability of oto-endoscopic grading of the thickness of the perforation margin was validated using an ANOVA analysis, based on the ratio of the LCI scan thickness as determined using the OCT system to 100 μm, the thickness of the normal TM on OCT (T value). Receiver operating characteristic (ROC) curves were plotted together with the areas under the curves (AUCs) to estimate the sensitivity and specificity of the OCT system as a diagnostic tool in evaluations of the perforation margin. An AUC of 1.0 defines an ideal test, and an AUC of 0.5 a test of no diagnostic value. The data were analyzed using SPSS version 18.0 (SPSS Inc., Chicago, IL). A p value <.05 was considered to indicate statistical significance.

Results

OCT images were successfully acquired in 85 of the 120 patients (70.8%). The diagnoses of Eighty-five patients were COM (N = 59), COM with cholesteatoma (N = 8), adhesive OM (N = 7), OME (N = 6), and other pathologies (N = 5). Among 85 patients, 24 patients (COM, N = 23; COM with cholesteatoma, N = 1) underwent an OCT examination postoperatively and seven patients both preoperatively and postoperatively. The OCT images acquired for the rest 35 patients with a narrow EAC (N = 20), cerumen impaction (N = 4), and poor cooperation (N = 11) were rarely informative, so excluded from analysis.

Evaluation of tympanic membrane perforation

A perforated TM was visible in 36 patients by OCT, with the images providing information about the characteristics of the perforation. The perforation margins differ according to the extent of inflammation and the cause of the perforation. In OM patients with early-stage or

traumatic TM perforation, the margin is sharp and thin on the video-camera image and the thickness of the TM shown on the LCI scan is similar to that of a normal TM. As inflammation and fibrosis progress, the margin of the perforation as seen on the video-camera image is blunted and thickened, a finding confirmed on 2D-OCT. The change is identified on the LCI scan as two peaks of decreasing intensity.

The thickness of the perforation margins was evaluated by oto-endoscopy and the patients were divided accordingly into three groups: borderline thickening, diffuse thickening, and fibrous band formation (Figure 2). The thickness of the perforation margin was then measured by LCI scan (Figure 2). The results were evaluated by three otologists blinded to the OCT information of the patients. The thickness was graded by consensus. The distribution of each group according to the oto-endoscopic findings and T value is shown in Table 2. The mean T values of the three groups as determined by LCI scan were 2.15 ± 0.65 (borderline thickening group), 3.02 ± 0.13 (diffuse thickening group), and 3.98 ± 0.13 (fibrous band formation group), which showed significant difference ($p = .002$). This means that the evaluation of the perforation margin using oto-endoscopy could be reliable based on objective measurement by OCT image.

Cut-off values for the T value were estimated in an AUC analysis. First, the ROC curve for the T value between the borderline thickening group and the other two groups (diffuse thickening and fibrous band formation groups) was plotted. The AUC was 0.811 ± 0.070 ($p = .003$). The sensitivity and the specificity were 64% and 78%, respectively, when the cut-off value of the T value was set to 2.80, obtained by adding the standard deviation from the mean value of the borderline thickening group. The ROC curve for the T value between the fibrous band formation group and the other two groups (borderline thickening and diffuse thickening groups) was similarly plotted. The AUC was 0.822 ± 0.070 ($p = .002$). At a cut-off value for the T value of 3.85, obtained by subtracting the standard deviation from the mean value of the fibrous band formation group, the sensitivity and the specificity were 55% and 84%, respectively.

Evaluation of tympanic membrane retraction

Retraction of the TM is observed in COM, OME, and early-stage adhesive OM. It is also frequently detected postoperatively. If the retraction progresses medially, the inner surface of the TM attaches to the middle ear mucosa, which is then replaced by fibrous tissue, hence the name adhesive OM. Because in these patients, the TM is connected to the middle ear mucosa, both the 2D and the LCI OCT evaluations will show iso-intensity following the initial peak.

The extent of retraction in 40 TMs was graded oto-endoscopically by three otologists blinded to the OCT information of all patients: Grade A1 was defined as retraction with residual space between the TM and middle ear mucosa; grade A2 as distinguishable contact between the TM and middle ear mucosa; and grade A3 as adhesion between the TM and bony structures, with the loss of the middle ear mucosa (Figure 3). Grading was by consensus of all three otologists and was performed by comparing the 2D-OCT and LCI scans with the oto-endoscopic grading (Figure 3 and Table 3). Each oto-endoscopically

based grade was divided into OCT-based grades. The rate of concordance between them was the lowest in grade A2 (40%).

Evaluation of postoperative outcomes

The OCT system allowed postoperative healing of the TM and middle ear cavity to be monitored. Tympanoplasty allows the repair of a perforated TM and thus the eradication of middle ear pathology. In this procedure, the temporalis fascia is generally used as graft material. As the healing process evolves, the temporalis fascia becomes thin and achieves continuity with the remaining normal TM. Figure 4 shows the findings in patients who underwent tympanoplasty. Preoperatively, the video-camera images and 2D-scan revealed TM perforation with blunt margins (Figure 4(A,C)). Postoperatively, perforation was replaced by the inserted temporalis fascia, with the remaining normal TM showing complete continuity and appropriate tension (Figure 4(B,D)).

Discussion

Although the penetration depth of OCT is limited to 2–3 mm, its non-invasive, high-resolution, real-time cross-sectional image acquisition ability is an important advantage compared to other TM imaging methods. OCT reveals TM thickness and allows the accurate evaluation of middle ear structures, including in patients with an intact TM. Detailed information on the pathologic findings can be acquired easily in an outpatient setting, which is not possible using an oto-endoscope. Because OCT can generate real-time images with a resolution of a few micrometers, it is a powerful modality for the diagnosis and monitoring of conditions of the middle ear.

Since the first report of the use of OCT technology for middle ear surgery, by Beyer et al. in 2001 [13], OCT has been used in clinical otorhinolaryngological practice and research. However, while micro-anatomic features within the cochlea were identified in several studies [14,15], clinical investigations of OCT were not robust due to technological and ethical limitations. Consequently, most research consisted of the ex vivo imaging of cadaveric temporal bone [16].

Recently, several studies using handheld OCT systems have been reported. Nguyen et al. described the use of OCT to detect and quantify the microstructure of the biofilm in the human middle ear [17]. Their study focused on both the early detection of these biofilms and their classification algorithms using an LCI/OCT otoscope system. Monroy et al. [18] used a handheld OCT system to measure TM thickness in pediatric patients and provided new metrics for differentiating normal, acute, and chronic OM. Hubler et al. [19] developed an OCT system for the real-time automated measurement of *in vivo* TM thickness including the presence or absence of a middle ear biofilm.

In the current study, two typical pathologies of the TM, perforation and retraction, were evaluated using a handheld OCT device. To adjust for individual differences in TM thickness, the T value was calculated using the normal TM thickness measured by OCT as a reference. The differences in the T values of the different oto-endoscopic grades were significant and the reliability of oto-endoscopic evaluation was proved by objective

measurement using OCT image, which could demonstrate the complementary role of an OCT system as an objective measurement tool. For example, in the preoperative evaluation of the perforation margin, the *T* value could be helpful for inferring disease duration, inflammatory status, and thus in counseling patients.

Unlike TM perforation, the grading of TM retraction was incongruent between the oto-endoscopic and OCT exams. In particular, the rate of concordance among examiners (40%) was lowest for grade A2 retractions as assessed on the oto-endoscopic exam. OCT system is able to provide the tomographic information inside the TM in outpatient clinic, which is one of the most beneficial advantages of OCT-based otoscope. Intermediate stages of TM retraction can be indistinguishable by oto-endoscopy, in which case OCT grading may aid in deciding the appropriate time to perform surgical repair. In addition, correlation analysis between preoperative retraction grade using oto-endoscope/OCT system and intraoperative grade using surgical microscope could be an important issue validating the efficacy of OCT system.

OCT could also be used to monitor postoperative healing of the TM, which could be a unique feature over conventional otoscopy. The continuity between the inserted graft and the margin of remnant TM could be identified tomographically and thinning change of graft followed up serially.

Studies using either the OCT system alone [20] or the OCT system together with other techniques [17,18] have been reported. A whole-TM examination using an oto-endoscope is a prerequisite for acquiring images of the region of interest when the OCT system is used alone. In the current study, the fiber-optics and micro-optics within the sample arm were highly amenable to integration with a video camera, allowing non-invasive acquisition of LCI/2D data *in vivo*. By combining the OCT system with the high-quality video camera, simultaneous evaluation of the whole TM and distinct regions of interest was possible.

Although the probe can easily be inserted through the EAC with the aid of a video camera, the acquisition of OCT images is difficult in narrow and curved EACs. The rate of successful acquisition of OCT images in this study was 70.8% (85/120). Among the 35 TMs for which OCT images were not acquired, 20 examinations were hindered by the diameter and curvature of the EAC. In the case of narrow and curved EAC, the anterior portion of the TM may be out of range of the probe even when a small speculum is used. The size reduction of speculum suitable for narrow and curved EACs would improve the performance of the OCT.

The OCT system has several other limitations. The thickness of a TM cannot be measured by opacity due to sclerotic plaque or cartilage replacement after surgery. In addition, the patient’s heartbeat, breathing, or other types of movement may disturb the acquisition of clear images. Upgrading the speed of signal processing and a swept-source-based set-up could improve the depth range and acquisition rate, allowing the handheld OCT system to acquire real-time images without motion artifacts in any area within the field of view. This is especially important in pediatric patients, who may not tolerate immobilization during the otoscopic examination.

Conclusion

This work presents the clinical characteristics of the TMs as described using a handheld otoscope-type OCT device. The imaging results were compared to those obtained with an oto-endoscope to evaluate the capabilities of the OCT system. In that the handheld OCT-based otoscope uniquely and non-invasively provides the cross-sectional information including thickness of the perforation margin and the extent of retraction in the outpatient clinic, it could be an objective tool complementary to conventional otoscope for patient care.

Acknowledgments

Funding

This work was financially supported by the Development of Microsurgical Apparatus based on 3D Tomographic Operating Microscope' funded by the Ministry of Trade, Industry & Energy (MI, Korea) (No. 10047943), and Bioengineering Research Partnership grant from the U.S. National Institutes of Health (1 R01 EB013723). This research was supported by Basic Science Research Program through the National Research Foundation of Korea (NRF) funded by the Ministry of Science, ICT & Future Planning (NRF-2015R1C1A1A02036457).

References

1. Revai K, Dobbs LA, Nair S, et al. Incidence of acute otitis media and sinusitis complicating upper respiratory tract infection: the effect of age. Pediatrics. 2007; 119:e1408–e1412. [PubMed: 17545367]
2. Martines F, Bentivegna D, Maira E, et al. Risk factors for otitis media with effusion: case–control study in Sicilian schoolchildren. Int J Pediatr Otorhinolaryngol. 2011; 75:754–759. [PubMed: 21514964]
3. Neff MJ. AAP, AAFP, AAO-HNS release guideline on diagnosis and management of otitis media with effusion. Am Fam Physician. 2004; 69:2929–2931. [PubMed: 15222658]
4. Neff MJ. AAP, AAFP release guideline on diagnosis and management of acute otitis media. Am Fam Physician. 2004; 69:2713–2715. [PubMed: 15202704]
5. Park M, Lee JS, Lee JH, et al. Prevalence and risk factors of chronic otitis media: the Korean national health and nutrition examination survey 2010–2012. PLoS One. 2015; 10:e0125905. [PubMed: 25978376]
6. Nguyen CT, Tu H, Chaney EJ, et al. Non-invasive optical interferometry for the assessment of biofilm growth in the middle ear. Biomed Opt Express. 2010; 1:1104–1116. [PubMed: 21258533]
7. Cho NH, Lee SH, Jung W, et al. Optical coherence tomography for the diagnosis and evaluation of human otitis media. J Korean Med Sci. 2015; 30:834. [PubMed: 26019479]
8. MacDougall D, Farrell J, Brown J, et al. Long-range, wide-field swept-source optical coherence tomography with GPU accelerated digital lock-in Doppler vibrography for real-time, *in vivo* middle ear diagnostics. Biomed Opt Express. 2016; 7:4621–4635. [PubMed: 27896001]
9. Lohmann G, Bohn S, Muller K, et al. Image restoration and spatial resolution in 7-tesla magnetic resonance imaging. Magn Reson Med. 2010; 64:15–22. [PubMed: 20577978]
10. Yushchenko DA, Schultz C. Tissue clearing for optical anatomy. Angew Chem Int Ed. 2013; 52:10949–10951.
11. Jung W, Kim J, Jeon M, et al. Handheld optical coherence tomography scanner for primary care diagnostics. IEEE Trans Biomed Eng. 2011; 58:741–744. [PubMed: 21134801]
12. Cho NH, Park K, Wijesinghe RE, et al. Development of real-time dual-display handheld and bench-top hybrid-mode SD-OCTs. Sensors (Basel). 2014; 14:2171–2181. [PubMed: 24473286]
13. Beyer W, Tauber S, Kubasiak S, et al. Optical coherence tomography of middle ear structure. Med Laser Appl. 2001; 16:135.
14. Tona Y, Sakamoto T, Nakagawa T, et al. *In vivo* imaging of mouse cochlea by optical coherence tomography. Otol Neurotol. 2014; 35:e84–e89. [PubMed: 24448302]

15. Gao SS, Xia A, Yuan T, et al. Quantitative imaging of cochlear soft tissues in wild-type and hearing-impaired transgenic mice by spectral domain optical coherence tomography. Opt Express. 2011; 19:15415–15428. [PubMed: 21934905]

16. Pitris C, Saunders KT, Fujimoto JG, et al. High-resolution imaging of the middle ear with optical coherence tomography: a feasibility study. Arch Otolaryngol Head Neck Surg. 2001; 127:637–642. [PubMed: 11405861]

17. Nguyen CT, Jung W, Kim J, et al. Noninvasive *in vivo* optical detection of biofilm in the human middle ear. Proc Nat Acad Sci USA. 2012; 109:9529–9534. [PubMed: 22645342]

18. Monroy GL, Shelton RL, Nolan RM, et al. Noninvasive depth-resolved optical measurements of the tympanic membrane and middle ear for differentiating otitis media. Laryngoscope. 2015; 125:E276–E282. [PubMed: 25599652]

19. Hubler Z, Shemonski ND, Shelton RL, et al. Real-time automated thickness measurement of the *in vivo* human tympanic membrane using optical coherence tomography. Quant Imaging Med Surg. 2015; 5:69–77. [PubMed: 25694956]

20. Djalilian HR, Ridgway J, Tam M, et al. Imaging the human tympanic membrane using optical coherence tomography *in vivo*. Otol Neurotol. 2008; 29:1091–1094. [PubMed: 18957904]

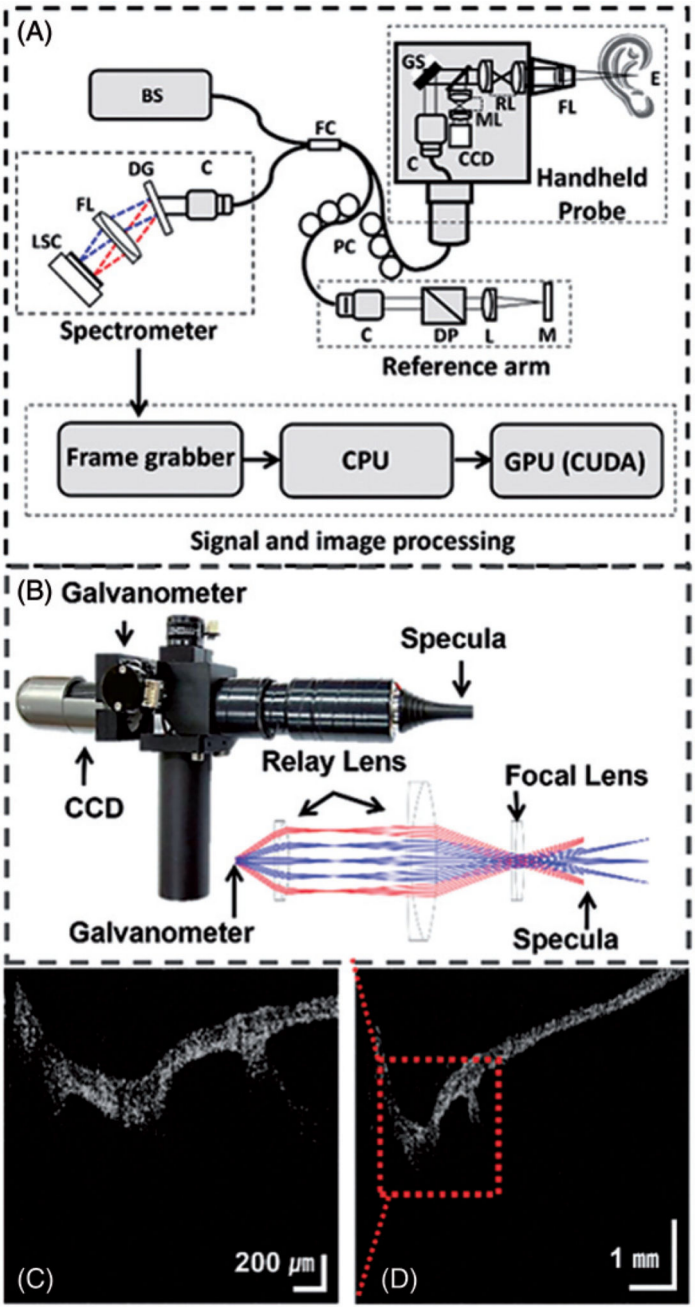

Figure 1.

Schematic of the handheld optical coherence tomography (OCT)-based otoscope and OCT images. (A) The handheld OCT device using a spectral domain (SD)-OCT system. (B) The handheld OCT probe and ZEMAX simulation. (C) Two-dimensional (2D) OCT image of the normal tympanic membrane using a conventional standard OCT system with a scanning range of 2 mm [rectangles in (D)]. (D) 2D image using an improved large-field OCT system with a scanning range of 7 mm. BS: broadband source; C: collimator; CCD: charge-coupled device; CPU: central processing unit; CUDA: compute unified device architecture; DG: diffraction grating; DP: dispersion compensation unit; E: ear; FC: fiber coupler; FL:

focusing lens; GPU: graphics processing unit; GS: galvanometer scanners; L: lens; LSC: line-scanning camera; M: mirror; ML: magnifier lens; PC: polarization controllers; RL: relay lens; ST: specula tip.

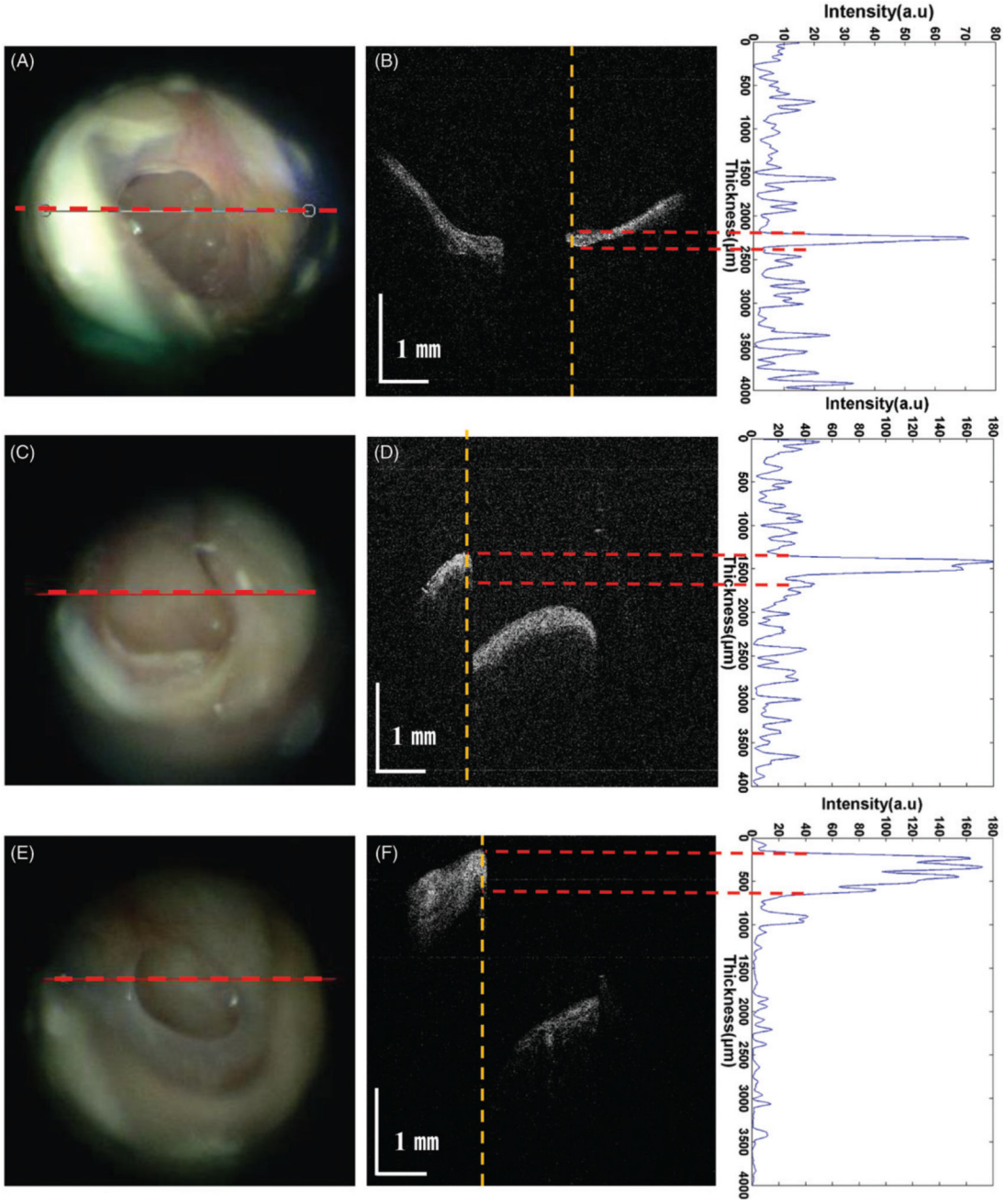

Figure 2.

Oto-endoscopic and OCT images used to measure the thickness of the tympanic membrane perforation margin. (A) Oto-endoscopic image showing borderline thickening. (B) OCT B-scan image (left) and OCT LCI scan profile (right) acquired along the red dotted lines in (A). (C) Oto-endoscopic image of diffuse thickening. (D) OCT B-scan image (left) and OCT LCI scan profile (right) acquired along the red dotted lines in (C). (E) Oto-endoscopic image of fibrous band formation. (F) OCT B-scan image (left) and OCT LCI scan profile (right) acquired along the red dotted lines in (E).

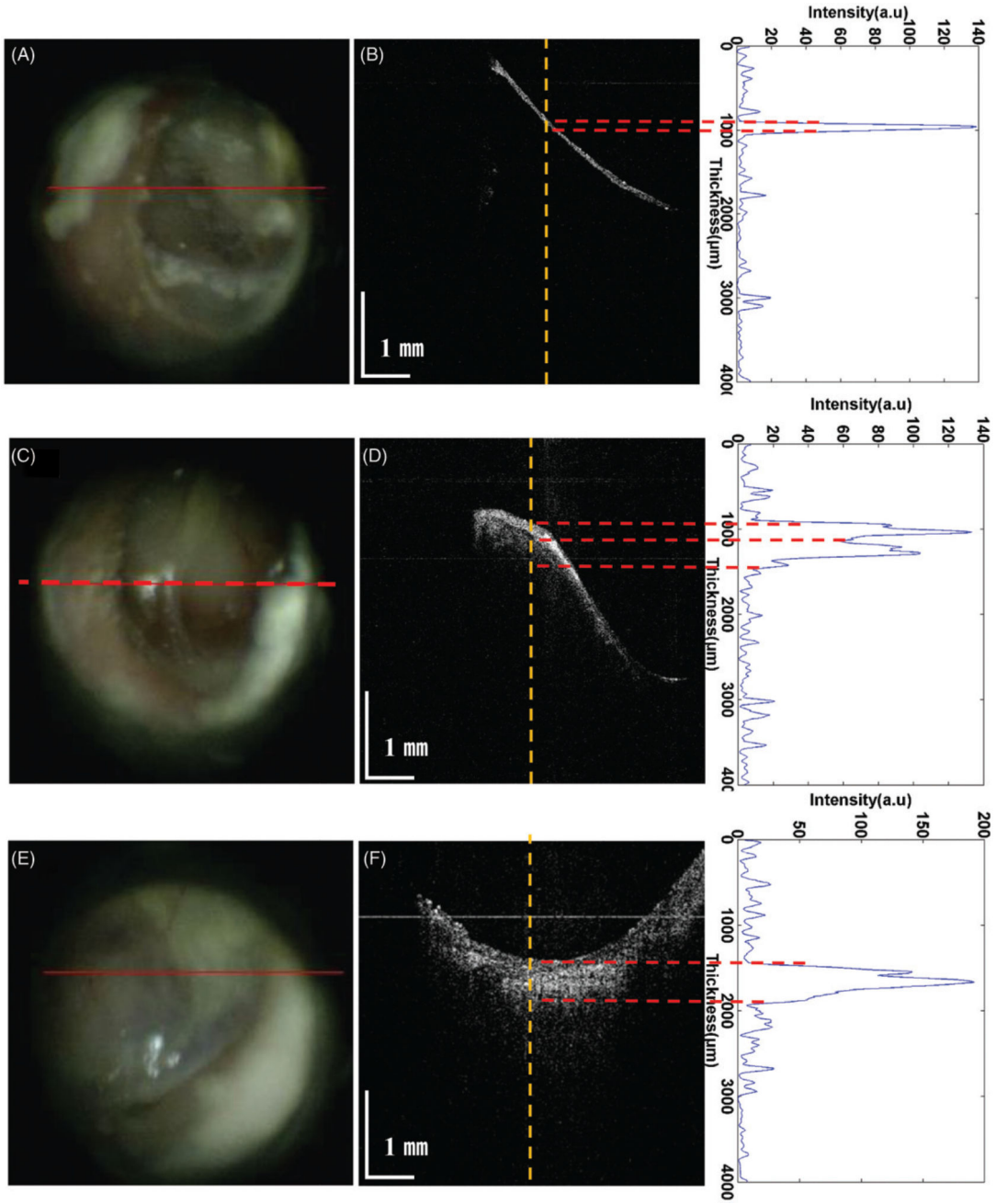

Figure 3.

Oto-endoscopic and OCT images used in the evaluation of tympanic membrane retraction. (A), (C), and (E) Oto-endoscopic images. The red line indicates the OCT scanning range. (B), (D), and (F) OCT B-scan image (left) acquired along the red line and OCT LCI scan profile (right) acquired along the yellow dotted lines. The red dotted lines in (B) represent the LCI scan profile of the retraction showing the residual space between the TM and middle ear mucosa. The red dotted lines in (D) represent the LCI scan profile showing distinguishable contact between the TM and middle ear mucosa. The red dotted lines in (F)

represent the LCI scan profile of adhesion between the TM and bony structures, with the loss of the middle ear mucosa.

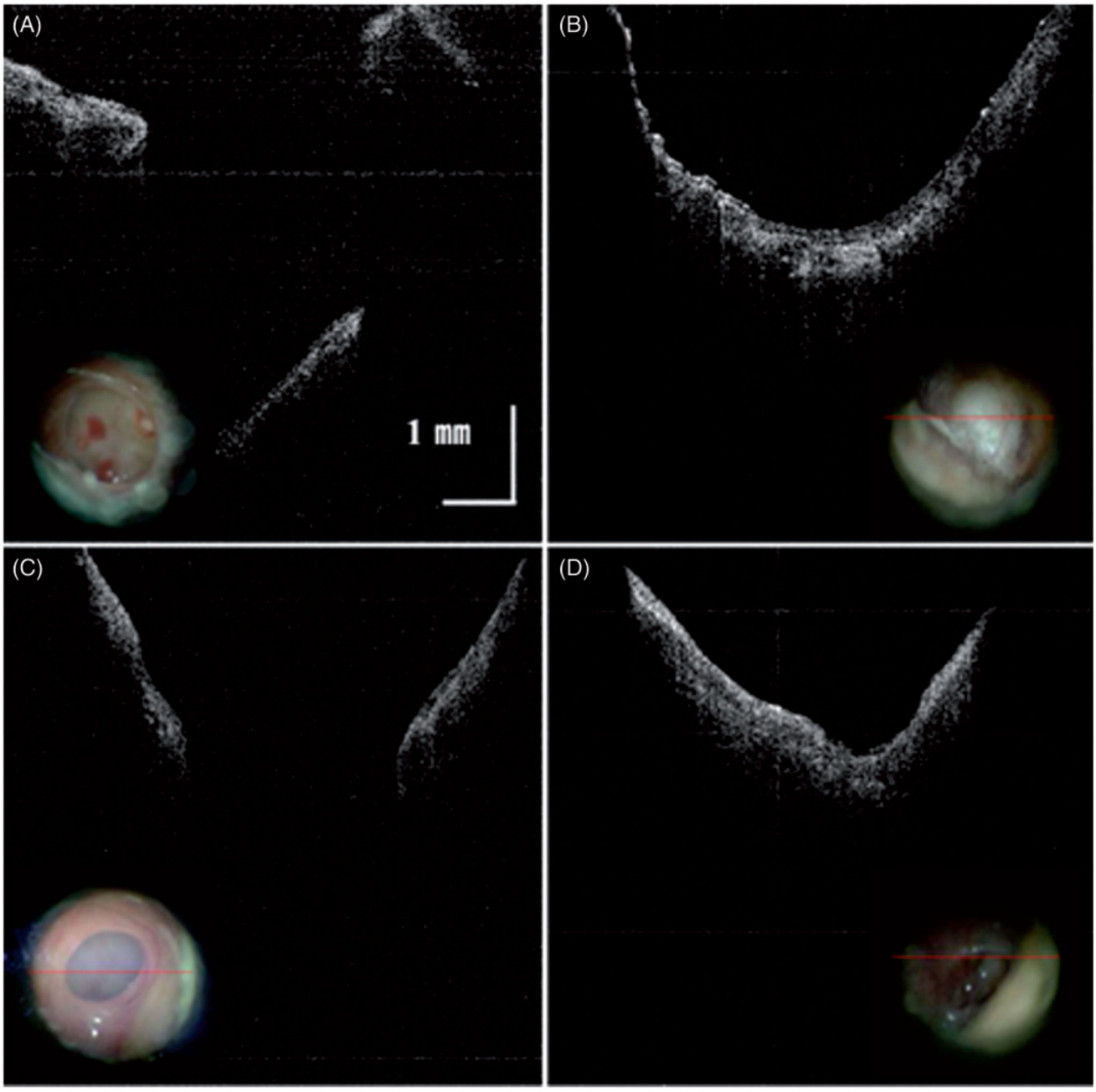

Figure 4.
OCT and oto-endoscopic images in the monitoring of postoperative healing of the tympanic membrane. OCT and oto-endoscopic (inset) images (A and C) before and (B and D) after tympanoplasty.

Table 1

Demographic characteristics of patients.

M:F (*N*)	37:83
Right:left (*N*)	55:65
Mean age (years)	50.6 ± 14.2
Diagnosis (*N*)	Chronic otitis media (86)
	Chronic otitis media with cholesteatoma (12)
	Adhesive otitis media (8)
	Otitis media with effusion (8)
	Others (6)

M: male; F: female; N: number.

Table 2

Distribution and T grade of patients according to oto-endoscopic findings of perforation margin.

Oto-endoscopic finding (*N*)	Mean *T* value	*p* Value
Borderline thickening (11)	2.15 ± 0.65	
Diffuse thickening (14)	3.02 ± 0.13	.002
Fibrous band formation (11)	3.98 ± 0.13	

N: number; J score, the ratio of LCI scan thickness to 100 μm.

Table 3

Rate of concordance between grades by oto-endoscope and OCT.

Grade by oto-endoscope (*N*)	Grade by OCT scan (*N*)	Rate of concordance (%)
A1 (9)	A1 (5), A2 (3), A3 (1)	5/9 (55.6)
A2 (15)	A1 (4), A2 (6), A3 (5)	6/15 (40)
A3 (16)	A2 (4), A3 (12)	12/16 (75)

N: number; OCT: optical coherence tomography; A1: retraction with residual space between the TM and middle ear mucosa; A2: distinguishable contact of TM and middle ear mucosa; A3: adhesion between the TM and bony structures with the loss of middle ear mucosa.